ARTICLES
https://doi.org/10.1038/s41557-021-00713-2
nature chemistry

Cyclic polyacetylene

Zhihui Miao[1,2], Stella A. Gonsales[1], Christian Ehm[3], Frederic Mentink-Vigier[4], Clifford R. Bowers[1], Brent S. Sumerlin[2]✉ and Adam S. Veige[1,2]✉

Here we demonstrate the synthesis of cyclic polyacetylene (c-PA), or [∞]annulene, via homogeneous tungsten-catalysed polymerization of acetylene. Unique to the cyclic structure and evidence for its topology, the c-PA contains >99% *trans* double bonds, even when synthesized at −94 °C. High activity with low catalyst loadings allows for the synthesis of temporarily soluble c-PA, thus opening the opportunity to derivatize the polymer in solution. Absolute evidence for the cyclic topology comes from atomic force microscopy images of bottlebrush derivatives generated from soluble c-PA. Now available in its cyclic form, initial characterization studies are presented to elucidate the topological differences compared with traditionally synthesized linear polyacetylene. One advantage to the synthesis of c-PA is the direct synthesis of the *trans-transoid* isomer. Low defect concentrations, low soliton concentration, and relatively high conjugation lengths are characteristics of c-PA. Efficient catalysis permits the rapid synthesis of lustrous flexible thin films of c-PA, and when doped with I_2, they are highly conductive (398 (±76) Ω^{-1} cm^{-1}).

Credited with formulating the structure of benzene as a cyclic six-membered ring possessing alternating single and double bonds, Kekulé forever altered the way chemists think about the composition of molecules[1,2]. Kekulé used the term 'affinity' to describe what we know today as bonds. In the following translated quote[2], he expresses the composition of benzene and the nature of alternating single and double bonds:

> "they combine alternately by one and by two affinities. In fact, six carbon atoms by combining according to this law of symmetry will give a group, which, considered as a chain open, will still have eight unsaturated affinities. If we admit, on the contrary, that the two atoms which terminate this chain combine with each other, we will have a closed chain"

This intellectual leap was important, as an understanding of the composition of atoms and the existence of electrons was not available to Kekulé at the time. It was not until 1929 that Lonsdale elucidated the structure[3], and in 1931[4] Hückel formalized the concept that cyclic rings having $(4n+2)\pi$ electrons exhibit aromatic behaviour. With the goal of exploiting the potential properties imparted by delocalized electrons, chemists have sought to synthesize large rings[5]. Even after 150 years, new principles of this composition of matter continue to emerge, including recent discoveries of global three-dimensional aromaticity[6].

[*n*]Annulenes are ring compounds with the same empirical formula as benzene, $C_{2m}H_{2m}$, where *n* is the number of carbon atoms, 2*m*. Sondheimer isolated [18]annulene in 1959[7] and [30]annulene in 1960[8,9]. Synthetically impressive, it is remarkable that [30]annulene is isolable. Unable to challenge the limits of aromaticity, ring size, and the properties of large aromatic rings of basic formula $(CH)_n$, no larger annulene rings were reported over the past 60 years, although theoretical treatments of annulenes with *n* values of 42, 54, and 66 have been performed[10]. Using Hartree–Fock and density functional theory, Choi and Kertesz[11] determined that when the highest occupied molecular orbital (HOMO)–lowest unoccupied molecular orbital (LUMO) gap decreases, a transition from delocalized to localized structures occurs at $4n+2=30$. An important property expected for an infinitely large annulene is electrical conductivity. [∞]Annulene (where $n>100$) should be semiconducting, just like its famous linear derivative polyacetylene (PA), first synthesized by Natta et al. in 1958[12]. Extensively studied[13], linear polyacetylene (l-PA) is a remarkable compound. Questioned recently, the true nature of the composition of the 'as synthesized'[14] linear polyacetylene remains[15].

Berets and Smith first reported the doping of PA in 1968[16], but it was Shirakawa and Ikeda[17] who synthesized free-standing films of *cis–transoid*-PA at −78 °C using $Ti(O^nBu)_4/AlEt_3$. Heeger, MacDiarmid, and co-workers demonstrated that its p- and n-doped derivatives exhibit high electrical conductivity[18]. These collective discoveries paved the way for modern flexible electronics that exploit the semiconducting properties of polymers containing delocalized electrons across alternating single and double bonds, which now find application in sensors, electrochromic devices, optical and photonic devices, organic light-emitting diodes, and photovoltaic cells[19,20]. With the potential for increasing the conductivity by orders of magnitude when doped, an infinitely large pure [∞]annulene should be semiconducting. Herein we report a number of important discoveries, the first and foremost being the catalytic synthesis of [∞]annulene, or cyclic polyacetylene (c-PA), according to Fig. 1b. In addition, the high efficiency of catalyst **1**, with measured initial rates of 620,000 g mol_{cat}^{-1} h^{-1}, allow the use of ultralow (ca. ppm) catalyst loadings that produce highly conjugated c-PA with low (<1% by NMR) defects, low free-electron density (determined by EPR), and easy postsynthetic workup. Free-standing films, bulk polymer, and transiently soluble forms of c-PA are now attainable using catalyst **1**.

Results and discussion

Evidence for a cyclic topology. Although newly developed catalytic ring-expansion[21–28] methods are rapidly growing in the field, cyclic polymers are inherently difficult to synthesize. We recently reported the catalytic synthesis of cyclic polymers from alkynes[29]. Employing

[1]Department of Chemistry, University of Florida, Center for Catalysis, Gainesville, FL, USA. [2]Department of Chemistry, George and Josephine Butler Polymer Research Laboratory, Center for Macromolecular Science and Engineering, University of Florida, Gainesville, FL, USA. [3]Dipartimento di Scienze Chimiche, Università di Napoli Federico II, Naples, Italy. [4]National High Magnetic Field Laboratory, Tallahassee, FL, USA. ✉e-mail: sumerlin@chem.ufl.edu; veige@chem.ufl.edu

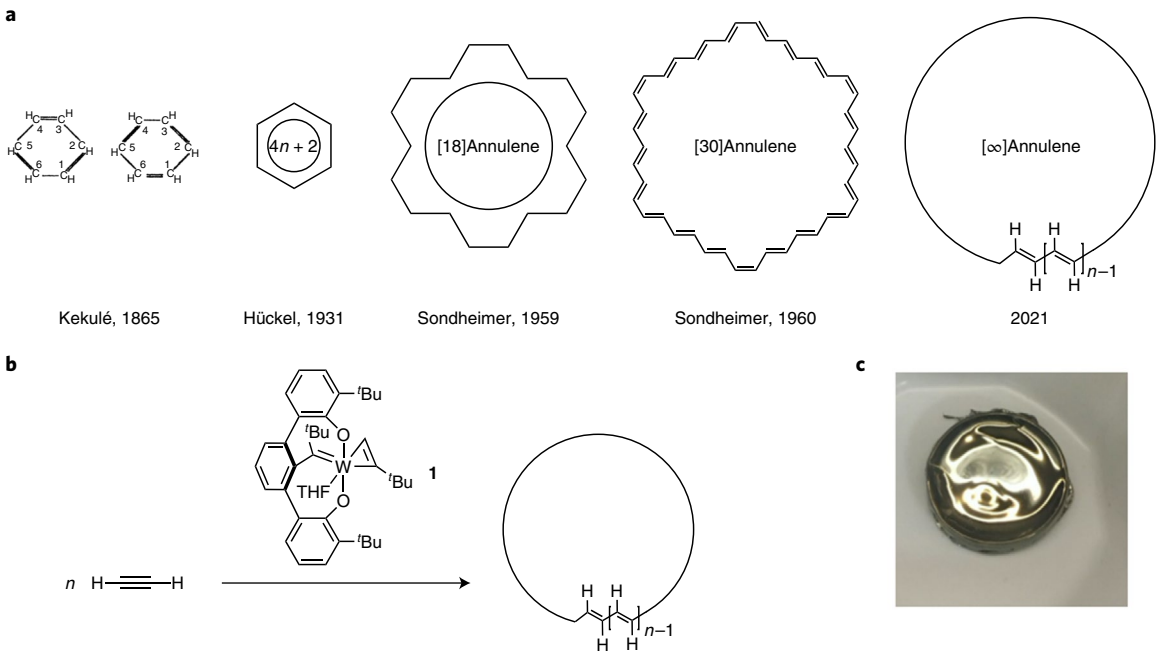

Fig. 1 | Historical development of isolable [*n*]annulenes. a, Historical development of annulenes spanning more than 150 years from Kekulé's assignment of benzene as a cyclic six-membered ring, to Hückel formulating the rules of aromaticity, to Sondheimer's synthesis of [30]annulene, to the current discovery described herein of c-PA. **b**, Exposing acetylene gas to catalyst **1** generates cyclic *trans–transoid*-PA. **c**, A photograph of a thin film of c-PA. The film grows within seconds of exposing a dilute solution of catalyst **1** to 1 atm of acetylene.

size-exclusion chromatography, dynamic light scattering, static light scattering, intrinsic viscosity, ozonolysis, rheology, and most recently atomic force microscopy (AFM) images of cyclic bottlebrush polymers on a surface[30], we confirmed the cyclic topology of the polymers produced using catalyst **1**[29,31–34]. In 2016, c-PA was synthesized in our labs by bubbling acetylene into a solution of catalyst **1** according to Fig. 1b. However, due to the polymer's well-known insolubility, air sensitivity, and lack of a melting point below its decomposition temperature, confirming a cyclic PA topology presented a formidable challenge. In its free-standing-film form, c-PA (Fig. 1c) has the same lustrous silvery appearance as l-PA. There is, however, an important difference between l-PA and the c-PA produced by catalyst **1**: l-PA, as synthesized using $Ti(O^nBu)_4/AlEt_3$ at −78 °C, results in *cis–transoid* double bonds[17]. The *cis* double bonds form as a consequence of the mechanism of a coordinated acetylene insertion into a growing polymer chain. In contrast, catalyst **1** produces c-PA with >99% *trans* double bonds even at −94 °C, a temperature too low to induce *cis–trans* isomerization[35,36]. It should be noted that a uniformly *trans* PA provides important insight and evidence for a cyclic topology and relates to the nature of configuration change and isomerization of [*n*]annulenes. Bates et al.[35] demonstrated the ability to produce *trans*-l-PA (95%) by altering the catalyst concentration, the ratio of Ti to Al, and the order of addition and timing; however, performed in our labs at −78 °C, the *cis* content increases to 62%, indicating that the ability of catalyst **1** to produce >99% *trans* PA is a unique feature. Vetting of the mechanism of ring expansion with catalyst **1** continues in our laboratories, but the observation of pure *trans*-c-PA appears to be unique to its cyclic topology (vide infra).

Heating *cis*-l-PA at 180 °C isomerizes the polymer to the *trans–transoid* form[17]. Figure 2 illustrates how the high barrier for isomerization is a consequence of having to rotate two C=C double bonds. Small annulenes undergo bond shift and configuration changes with barriers that permit their measurement in solution. For [16]annulene above −50 °C, planar bond shifting,

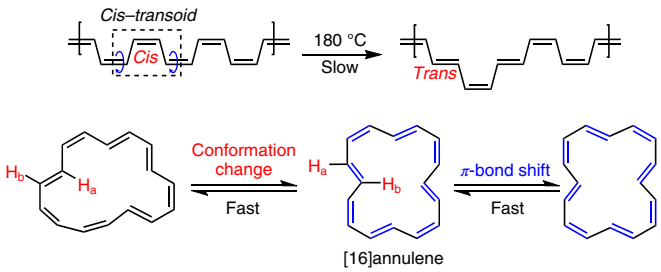

Fig. 2 | Isomerization for linear polyacetylene and [16]annulene. Top: isomerization of linear *cis–transoid*-PA to *trans–transoid*-PA requires heat treatment due to the high isomerization barrier to rotate C=C double bonds. Bottom: in contrast to linear conjugated molecules, annulenes (for example, [16]annulene) have low barriers to configuration changes, evidenced by ^{1}H NMR spectrsocopy of H_a and H_b, π-bond shifts and single bond rotations within the ring. Access to low barriers for isomerization enables large annulenes to rapidly adopt the more thermodynamically stable *trans* π-bond configuration.

degenerate conformational change, and configuration changes occur rapidly, resulting in a single resonance for the ring protons in its ^{1}H NMR spectrum[37]. Adding to this rapid exchange, tunnelling of the 16 carbon atoms was recently proposed[38]. Having access to a low-barrier π-bond shift differentiates linear and cyclic unsaturated compounds. Another important point is that as annulenes increase in size, the conformational constraint relaxes and the double bonds adopt the thermodynamically more stable *trans* form. For example, this idea was proposed for [30]annulene (Fig. 1a), and it has mainly *trans* bonds in its lowest energy configurations[8,9]. In short, c-PA can only exist in its *trans–transoid* configuration, and may even occur while still attached to the tungsten (W) centre, an outcome consistent with >99% *trans* double bonds in the c-PA produced with catalyst **1**.

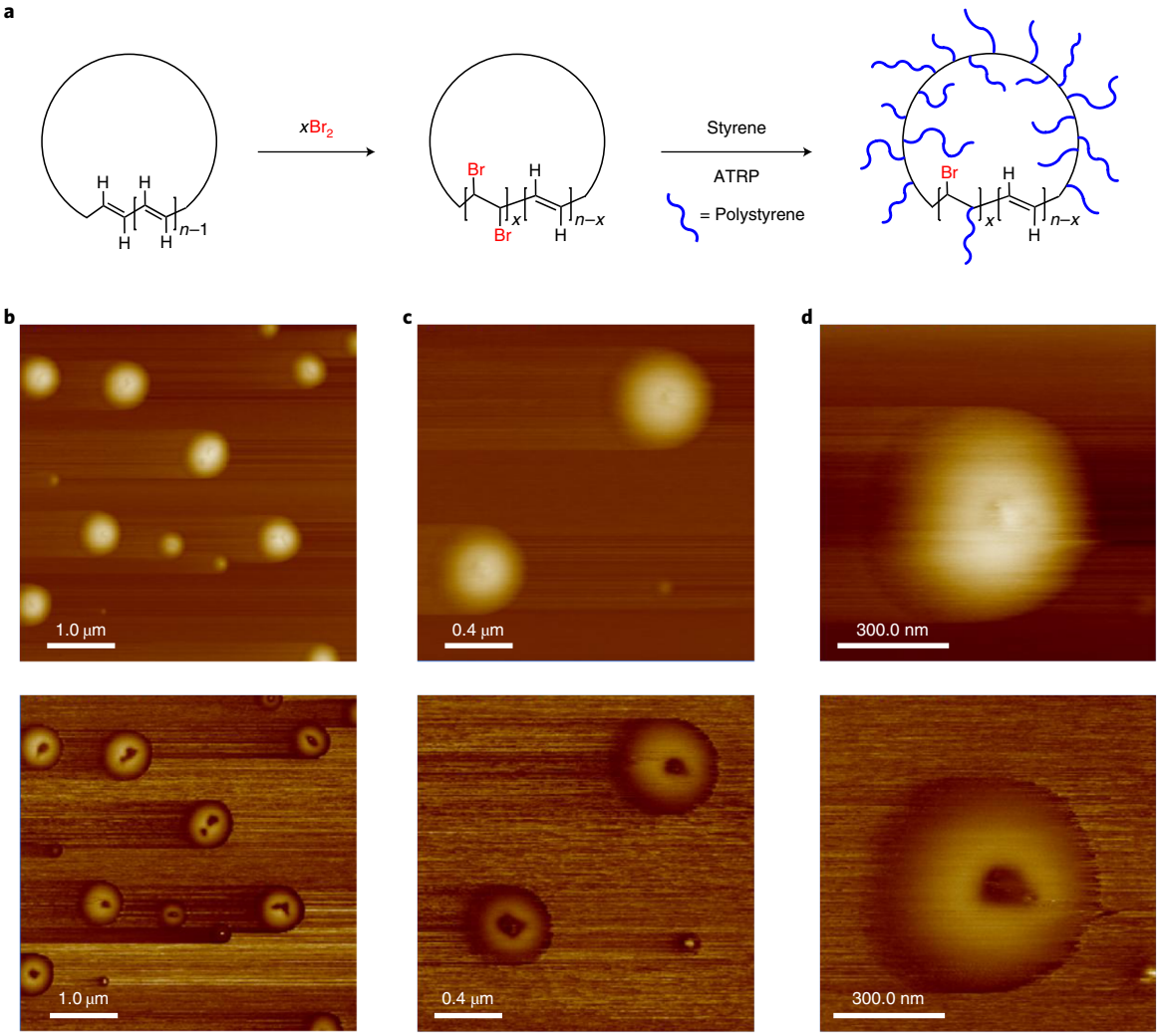

Fig. 3 | Evidence for a cyclic topology from AFM images of cyclic bottlebrushes spin-coated onto a mica surface. a, Reaction scheme for the synthesis of cyclic bottlebrushes via partial bromination of c-PA followed by grafting-from polymerization via ATRP with styrene. **b**–**d**, AFM height (top) and phase (bottom) images of cyclic bottlebrushes on different focused ranges.

Observation of an all-*trans* configuration is strong support for a cyclic topology, but it is not absolute evidence. Seeking to confirm the cyclic topology, we can exploit the properties of catalyst **1** that are distinctly different from conventional polymerization catalysts. Catalyst **1** permits polymerization at low temperatures and low concentrations, leading to temporarily soluble c-PA. Partial bromination of the backbone double bonds before precipitation followed by grafting-from polymerization via atom-transfer radical polymerization (ATRP) produces cyclic bottlebrush derivatives, according to Fig. 3a. Figure 3b–d depicts AFM images of the cyclic bottlebrush samples cast onto a mica plate surface. Timing, concentration, equivalents of Br_2 and extent of conversion during ATRP are all crucial for creating cyclic bottlebrushes that conclusively reveal their cyclic topology (see Supplementary Information for synthetic details). Importantly, cyclic structures result from multiple samples using different conditions, and the structures appear throughout the surface. These are the first images of postpolymerization derivatives of polyacetylene, regardless of topology.

Spectroscopic characterization of *trans–transoid*-c-PA. Catalyst **1** enables the synthesis of bulk, thin films and, as mentioned, temporarily soluble c-PA. For example, injecting a toluene solution (5 mg ml^{-1}) of catalyst **1** (400 μl) into an acetylene-saturated toluene solution (10 ml) at temperatures ranging from −94 to 65 °C produces c-PA as a black viscous gel that converts to a black powder after removing all volatiles and washing with pentane and THF. The formation of c-PA is rapid on exposing acetylene to catalyst **1**, with a measured initial activity of 620,000 g mol_{cat}^{-1} h^{-1} (Supplementary Fig. 5) at 25 °C. Alternatively, exposing a vial coated with toluene solution (400 μl) containing catalyst **1** (5 mg ml^{-1}) with an atmosphere of acetylene for 15 min at different temperatures ranging from −78 to 65 °C produces free-standing flexible and silvery films of c-PA (Supplementary Fig. 2). Another approach involves injecting a dilute THF solution of **1** (25 μl, 1.0 mg ml^{-1}) into a highly dilute acetylene/THF solution (3.00 ml, 0.03 mg ml^{-1}) at −20 °C to produce temporarily soluble c-PA. At all temperatures ranging from −94 °C to 65 °C, all the methods exclusively yield PA comprising >99% *trans* double bonds, as confirmed by infrared (IR) spectroscopy (Fig. 4a and Supplementary Figs. 1 and 3). Figure 4a depicts the remarkably clean IR spectra of thin films of c-PA produced at −78 °C (blue), 25 °C (orange), and 65 °C (black). The important features are the strong *trans* =C–H out-of-plane bending at 1,010 cm^{-1} and the weak =C–H stretching vibration at 3,010 cm^{-1}. Importantly, the IR spectrum of c-PA does not exhibit the end group terminal CH_2 or CH_3 stretches at 1,458 cm^{-1} and 1,378 cm^{-1} that are evident in the linear samples prepared using $Ti(O^nBu)_4/AlEt_3$ (Supplementary Fig. 7).

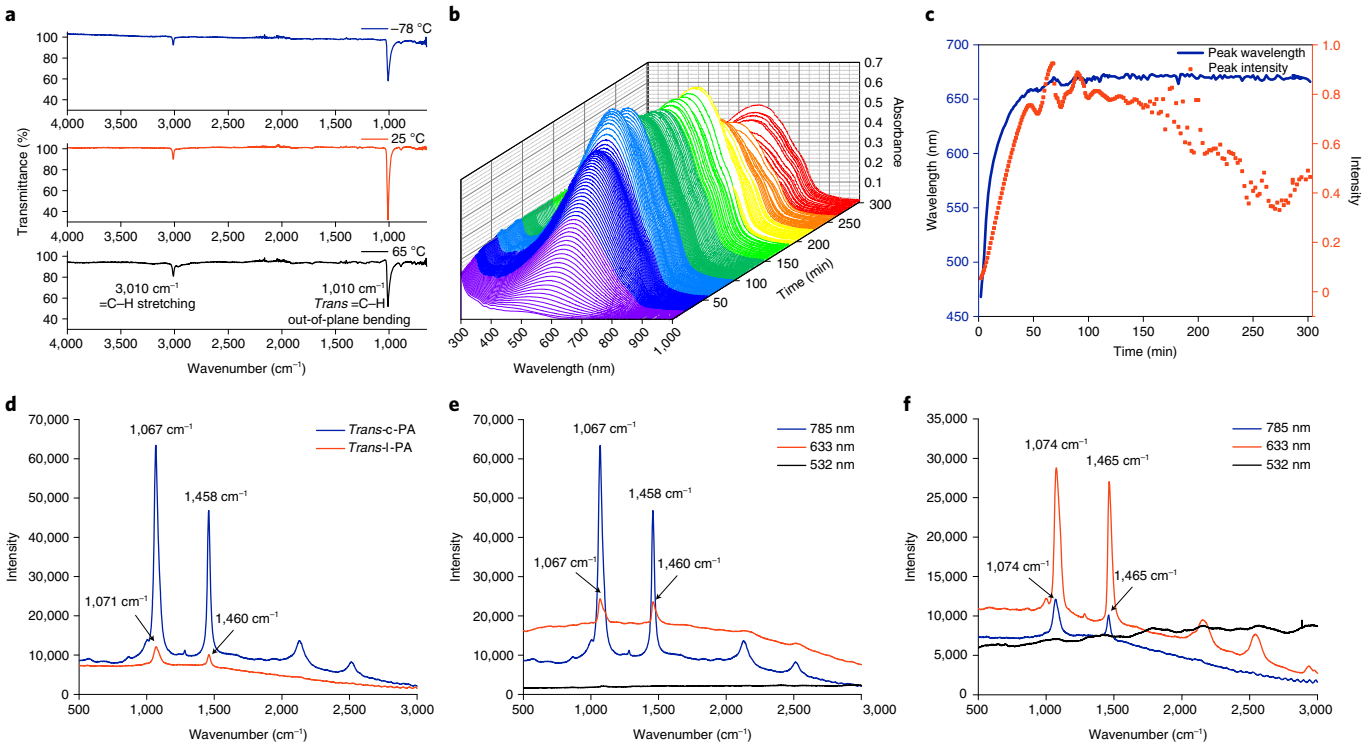

Fig. 4 | Spectroscopic characterization of c-PA. a, Due to the cyclic structure of the polymer or ring-expansion mechanism with catalyst **1**, the IR spectra of c-PA films produced at −78 °C (blue), 25 °C (orange), and 65 °C (black) exhibit strong *trans* =C–H out-of-plane bending at 1,010 cm^{-1} with no observable *cis* absorption at 750 cm^{-1}. **b**, The UV-vis spectra recorded during polymerization of acetylene with **1** in THF at −20 °C indicate the temporarily (5 h) soluble form of c-PA. **c**, The plot of λ_{max} and intensity versus polymerization time reveals an increase in both λ_{max} and intensity during the first 1 h of polymerization, suggesting the continuous formation of c-PA and a corresponding increase in conjugation. **d**, The Raman spectrum of *trans-transoid*-c-PA prepared at 25 °C exhibits a stronger signal with lower excitation energy (785 nm) than *trans-transoid*-l-PA prepared from $Ti(O^nBu)_4/AlEt_3$, suggesting more conjugated segments in c-PA. **e**, Raman spectrum of c-PA, which exhibits a narrow window of excitation and intense absorption under long-wavelength excitation of 785 nm (blue), compared with excitation at 633 nm (orange) and 532 nm (black). **f**, The Raman spectrum of l-PA, which exhibits more intense Raman signals when excited at 633 nm (orange) compared with 785 nm (blue) and 532 nm (black), suggests that c-PA has a relatively higher concentration of longer conjugation segments.

Raman, absorption, solid-state CP-MAS ^{13}C NMR, EPR, and morphology. Related to the discussion of conjugation and the very nature of the alternating double and single bonds in l-PA, Hudson[15] suggests the true nature of linear *trans*-PA is not one of an extended structure but rather finite segments of polyenes. Hudson argues that the zero-point energy vibration is above the transition state barrier separating the Peierls distortion and leading to alternating single and double bonds[15]. Thus, if PA could truly be synthesized, it would be metallic. Linear finite polyenes containing chain ends and cross-links give rise to Raman data showing C–C and C=C absorptions. An interesting phenomenon occurs for cyclic aromatics. As mentioned, for [*n*]annulenes where $n \geq 30$, an alternating structure of single and double bonds is strongly favoured. Raman spectra of thin films of c-PA feature C–C and C=C stretching vibrations at 1,067 cm^{-1} and 1,458 cm^{-1}, respectively (excitation wavelength 785 nm). The Raman frequency of the C=C stretch in *trans*-PA is markedly dependent on the excitation wavelength (Fig. 4d–f)[39], a result interpreted as a combination of the resonance Raman effect and the dependence of vibrational frequency and optical gap on the conjugation length of polyenes[39–41]. The dependence also suggests that the Raman signals arise from segments of different conjugation lengths in *trans*-PA[39]. Samples of l-PA are challenging to characterize due to inherent polydispersity[42], inhomogeneity[43], and coexistence of ordered and disordered phases[44,45].

Several different methods, including extrapolations from oligomers[41,46–48] and calculations based on different theories[40,49], were employed in previous studies to correlate the Raman frequencies and *trans*-PA conjugation lengths. Substituting the value of 1,458 cm^{-1} from c-PA into those equations[46–49] yields average conjugation lengths and lower limits between 30 and 43 bonds, including ~40 based on the approach established by Schrock and co-workers[47]. However, using Lichtmann, Fitchen, and Temkin's equation[41], the estimated conjugation length of c-PA is 114, similar to the linear PA produced by Xia et al. that exhibits a transition at 1,463 cm^{-1} (ref. [50]). According to Ikeda, Shirakawa, and co-workers, a C=C stretching vibration at 1,466 cm^{-1} (excitation wavelength 676.4 nm) corresponds to a conjugation length upper limit of ≥100 as well[39]. Considering that samples produced by **1** exhibit a red-shifted Raman absorption at 1,458 cm^{-1}, an estimate for the upper limit of 100 conjugated units is not unreasonable. Exciting c-PA at 532 nm does not produce a signal, while exciting at 633 nm results in significantly reduced absorption with minimal change in frequency (1,460 cm^{-1}) or line shape (Fig. 4e), which is indicative of a lower limit on the conjugation.

An ultraviolet–visible (UV–vis) spectrum of c-PA reveals a broad absorption with a λ_{max} (wavelength at strongest absorption) at 670 nm and allows for temporal monitoring of the polymerization in solution (Fig. 4b). Notoriously insoluble, only a few experiments have directly measured the UV–vis absorption of soluble PA. Xia et al. produced PA via sonication with the polymer exhibiting a λ_{max} at 636 nm (ref. [50]), and most recently Choi et al. produced a related conjugated PA with a λ_{max} at 651 nm (ref. [51]). Grubbs's ring-opening

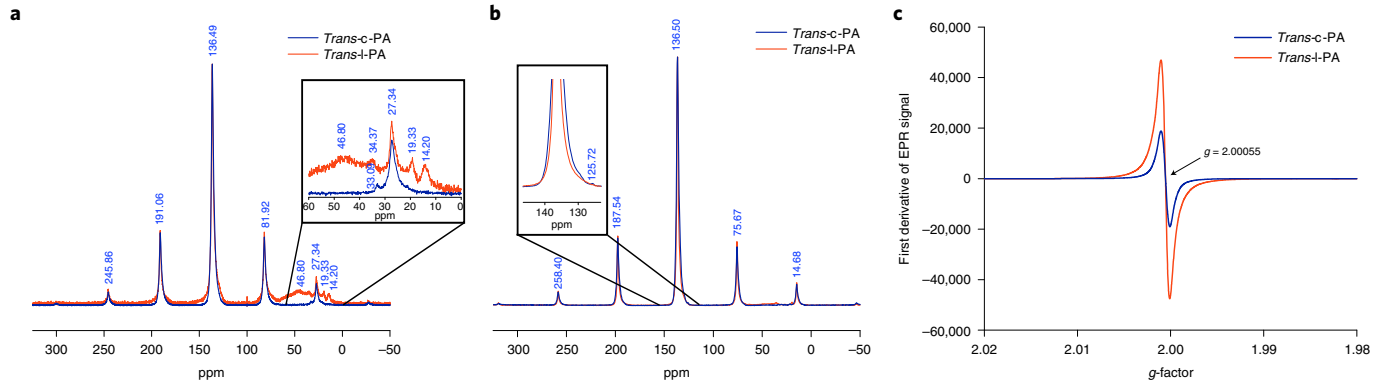

Fig. 5 | Spectroscopic characterization of c-PA. a, Resonances centred at 136.49 ppm in CP-MAS ^{13}C NMR spectra of *trans*-c-PA (blue) and *trans*-l-PA (orange) obtained at 25 °C confirm their *trans* configuration. c-PA exhibits much fewer (<1%) saturated carbon signals in the range from 15 to 70 ppm, indicating a lower defect concentration in c-PA compared with l-PA. The insert reveals chain end group ($-CH_2CH_3$ or $-CH_3$) signals at 34.47 and 14.20 ppm that are plainly evident in l-PA, whereas in the spectrum of c-PA, those signals are absent or beyond the detection limit. **b**, *Trans*-c-PA exhibits a significantly broader resonance in the MAS-DNP ^{13}C NMR spectrum (blue) obtained at 25 °C compared with *trans*-l-PA (orange), possibly due to its cyclic topology. **c**, Both *trans*-c-PA (blue) and *trans*-l-PA (orange) exhibit single narrow Lorentzian line shapes with a *g*-factor of 2.00055 in their EPR spectra (X band) obtained at 26.9 °C. *Trans*-l-PA has a soliton density of 1.28×10^{19} e^- g^{-1}, whereas *trans*-c-PA synthesized at 25 °C, without the need to isomerize at elevated temperatures, contains a lower soliton density of only 3.98×10^{18} e^- g^{-1}.

of substituted cyclooctatetraene produces substituted PA with a range of λ_{max} between 302 and 634 nm (ref. [52]). For perspective, Grubbs[53] and Schrock[46,54] were able to produce oligomers of PA and observed absorptions between 355 and 540 nm with distinct transitions that correspond to 10–20 double bonds. c-PA synthesized with **1** at −20 °C under dilute conditions is soluble for ~1 h. The broadness of the UV–vis absorption indicates a distribution of segments with different conjugation lengths[55,56]. In the first 1 h, the increase in both λ_{max} and intensity suggests the continuous formation of c-PA and a corresponding increase in conjugation length. After 47 min, the peak intensity starts to fluctuate and gradually decreases after 67 min as c-PA precipitates (Fig. 4c). c-PA produced by catalyst **1** exhibits the longest solution-phase absorption recorded with a λ_{max} reaching 670 nm and a tail extending to 950 nm. The 950 nm absorption tail is unusual for PA, and while its origin is not clear at this time, it may be inherent to the cyclic topology. Xia observed a blue shift when PA precipitates from the solution[50]. However, as c-PA starts to precipitate after 67 min, the λ_{max} remains at ~670 nm with no significant hypsochromic shift as the intensity decreases, suggesting c-PA maintains its high conjugation as it precipitates from solution. The absorption profile of c-PA is broad, but not unusual, as other experimental and theoretical studies also report a broad profile[39,57,58]. Eliminating the possibility that the broad absorption is due to scattering from particles suspended in solution, a UV–vis spectrum of a thin film of c-PA exhibits the same absorption profile (Supplementary Fig. 8), thus confirming the absorption is molecular in origin.

In agreement with high *trans* content of >99%, the cross-polarization magic-angle spinning (CP-MAS) ^{13}C NMR spectrum of c-PA in Fig. 5a exhibits a resonance centred at 136.49 ppm for *trans*-$(CH)_n$[59]. Consistent with a cyclic topology, the spectrum does not exhibit the CH_2 or CH_3 chain end group resonances at 34.47 and 14.20 ppm (ref. [60]), respectively, that are plainly evident in l-PA. The spectrum of l-PA contains a broad resonance between 15 and 70 ppm; attributed by others to defects, this resonance can arise from cross-linking or saturated bonds. Adopting a slower spinning speed, the resonances, which overlap at 27.34 ppm with the spinning sideband, separate and are observable in Supplementary Fig. 11. The minor impurity in the c-PA sample that resonates at 33.09 and 21.09 ppm can be due to saturation ($-CH_2-CH=CH$). As a rough estimate and evidence for low defects, the integration of sp^3 hybridized carbons is <1% in c-PA compared with 24% in l-PA.

Figure 5b presents preliminary MAS-DNP (for dynamic nuclear polarization)[61] ^{13}C NMR data revealing a clear difference between the two topologies of l-PA and c-PA. For the *trans* C=C bond at 136 ppm, c-PA exhibits a significantly broader resonance (width at half-height ~5 ppm for c-PA versus 2 ppm for l-PA). This line broadening is independent of the measurement temperature. For model PA compounds, Schrock demonstrated that ^{13}C resonances for C=C bonds in *cis*- and *trans*-l-PA rapidly converge to a value close to the one found for *cis*-l-PA (within ~5 units from the chain ends), indicating that the broadening in c-PA is not due to a distribution of small linear fragments[62]. In CP-MAS ^{13}C NMR experiments, Kaplan demonstrated that the *trans*-PA signal is sensitive to microstructural sequencing, while the *cis* is not[63]. During isomerization from *cis*-l-PA to *trans*-l-PA, the *trans*-l-PA signal line width narrows with increasing *trans* content. Clearly, c-PA has fewer structural defects than l-PA: the median length of *trans* sequences in c-PA is at least 49, a tenfold increase over the l-PA sample (determined from the ratio of the *trans*-PA signal versus *cis*-PA and sp^3-hybridized carbons). The observed broadening for the more perfect c-PA sample is incompatible with a linear topology and points towards its cyclic topology, although more studies are required to confirm this phenomenon.

Solitons (neutral defects) are inherent in *trans*-PA regardless of topology due to two energetically equivalent states arising from bond alternation and give rise to X-band EPR signals that are well studied[64–66]. Solitons are not present in thin films comprising linear *cis*-PA[67], since bond alternation results in inequivalent states (*trans–cisoid* and *cis–transoid*). However, on heating above 150 °C, *cis*-PA isomerizes to *trans*-PA, and an EPR signal develops that is characteristic of mobile, free π electrons (solitons). Figure 5c depicts the EPR spectra (26.9 °C) for *trans*-l-PA and c-PA. Agreeing well with earlier studies on *trans*-l-PA[64,66,68], both l-PA and c-PA exhibit single narrow Lorentzian line shapes with a *g*-factor of 2.00055, close to the free-electron value. The peak-to-peak linewidths ΔH_{pp} of l-PA and c-PA are 1.58(±0.03) and 1.54(±0.04) G, respectively, a typical width for the *trans* isomer of PA at ambient temperature. Quantitative measurement relative to TEMPO reveals that l-PA has one free electron for every 3,600 (±300) carbons, or 1.28×10^{19} e^- g^{-1}, a close fit to previous studies[64]. In contrast, c-PA synthesized at 25 °C contains only one free electron for every 11,600 (±900) carbons (or 3.98×10^{18} e^- g^{-1}).

Table 1 | Conductivities of c-PA films with different doping percentages of I_2

	Doping time (h)	Composition	Conductivity ($\Omega^{-1}cm^{-1}$)
trans-c-PA-1	0	$(CH)_n$	5.05 (±1.65) ×10^{-6}
trans-c-PA-2	1	$(CHI_{0.16})_n$	234 (±50)
trans-c-PA-3	3	$(CHI_{0.20})_n$	398 (±76)
trans-c-PA-4	24	$(CHI_{0.23})_n$	363 (±58)
trans-l-PA-1	0	$(CH)_n$	3.02 (±1.50) ×10^{-6}
trans-l-PA-2	3	$(CHI_{0.19})_n$	179 (±21)

One exciting feature of c-PA produced by catalyst **1** in its all-*trans* form at low temperatures is the opportunity to measure the inherent soliton concentration without the need for heating, an experiment never performed before. Remarkably, an EPR spectrum of a c-PA sample prepared at −78 °C and kept cold reveals only one free electron for every 119,100 carbons. Moreover, demonstrating the difference between the two topologies in parallel conditions, l-PA and c-PA were heated at 150 °C for 5 min before acquiring the EPR spectra. The linear sample results in $1e^-$ per 3,600 (±300) carbons; however, heating c-PA only results in $1e^-$ per 6,000 (±500) carbons, or an ~40% reduction in solitons. One explanation for this difference centres on the fact that chain ends repel solitons[69,70]. Without chain ends, solitons are free to diffuse over the entire length of a cyclic polymer, thus effectively lowering the inherent soliton concentration. Unfortunately, a direct comparison here is not possible since the composition of the two polymers (molecular weight and dispersity, *Đ*) is unmeasurable. The preliminary result of a 40% reduction in soliton concentration for c-PA versus l-Pa is intriguing and will be the subject of future interrogations.

Not expected to change, the solid-state morphology of c-PA is very similar to that of l-PA[13]. Supplementary Fig. 18 depicts the scanning electron microscopy images of the lustrous and dull sides of the thin films prepared with catalyst **1** at 25 °C. Presented at the same scale, it is obvious that the dull side of the film is loosely packed with larger fibrils, whereas the lustrous side contains dense fibrils with ~0.33 μm width. Energy-dispersive spectroscopy performed on c-PA reveals very low metal contamination (between 0.39 and 0.85 wt% W), whereas the l-PA sample contains 2.07 wt% Ti and 5.35 wt% Al (Supplementary Tables 3–5 and Supplementary Table 6). Despite the high quality of the c-PA produced with catalyst **1**, the stability of c-PA is identical to linear samples. Exposed to air, both l-PA and c-PA exhibit IR absorptions attributable to oxidation at the same rate, and thermal gravimetric analysis indicates that both have similar onset decomposition temperatures of 361 °C (Supplementary Figs. 21 and 22).

Electrical conductivity. The effect of chain ends on electrical resistivity and soliton formation in PA has been discussed in the literature[69,70]. Unfortunately, probing chain end effects requires l-PA and c-PA featuring similar defects, conjugation lengths, conjugation distribution and impurity content that is currently not possible. However, I_2-doped samples of c-PA exhibit conductivities at the higher end of the range (without chain alignment)[71,72] observed for l-PA prepared via Shirakawa's method. Table 1 lists the results of several electrical resistance measurements.

Kekulé formulated the composition of aromatic compounds (benzene) without modern spectroscopy. Absolute proof of the composition of benzene was not available but, importantly, Kekulé's hypothesis fit the available data. The insolubility preventing typical solution-phase size-exclusion chromatography and dynamic light scattering characterization, and the reactive nature of c-PA, created a similar challenge to provide absolute proof of its cyclic topology. In a way, characterizing c-PA presented some of the same challenges Kekulé confronted 150 years ago. Not available to Kekulé, AFM images of bottlebrush derivatives of c-PA provide irrefutable evidence for the cyclic topology. However, evidence supporting c-PA comes from other methods and data too, in particular, the unusual all-*trans* form of the polymer. Moreover, for all other polymerizations of substituted acetylenes with catalyst **1**, where solubility of the resulting polymer is not an issue, size-exclusion chromatography, dynamic light scattering, static light scattering, intrinsic viscosity, ozonolysis, rheology, and AFM images are consistent with a cyclic toppology[29,31–33]. l-PA produced using typical catalysts contains *cis* double bonds in accordance with an insertion mechanism and requires relatively extreme conditions (150–200 °C) to isomerize. However, due to the cyclic structure and access to low barriers, even at −94 °C, a temperature far too low to induce isomerization, catalyst **1** produces a polymer with >99% *trans–transoid* double bonds. The exclusive *trans* isomer fits with the fact that large annulenes undergo rapid configuration changes and double bond isomerization[37], whereas linear polyenes such as β-carotene have much larger barriers (the extrapolated experimental value is 22.4 kcal mol^{-1} (ref. [73]); the computed model value[74] is 22.9 kcal mol^{-1}). Another important point is that the thermal barrier for isomerization of l-PA is not constant during the isomerization. Initially, the barrier is estimated to be 17 kcal mol^{-1}, but as more and more isolated *cis* bonds remain, the barrier increase to 39 kcal mol^{-1} when 20% *cis* bonds remain. In contrast, c-PA isomerizes to greater than >99% at −94 °C. Eliminating the possibility of a radical-induced isomerization at low temperatures, polymerization in the presence of TEMPO does not change the *trans* outcome during the synthesis of c-PA (Supplementary Fig. 4). Finally, previously confirmed to have a cyclic topology, cyclic polyphenylacetylene produced with catalyst **1**, in contrast to c-PA, contains 90% *cis* double bonds[27]. The high *cis* content suggests that catalyst **1** inserts alkynes, as expected, via a traditional insertion mechanism, but the phenyl substituent must raise the barrier to isomerization, thus effectively trapping the *cis* stereochemistry.

In addition to the unique topology produced by catalyst **1**, c-PA has several properties that present exciting opportunities for further exploration. Catalyst **1** rapidly produces PA, with pristine films developing within seconds on contact with 1 atm of acetylene gas and ppm catalyst loadings. Catalyst **1** is highly active towards the polymerization of acetylene and, importantly, does not require copious equivalents of $AlEt_3$ cocatalyst. Simply washing (three to five times) with THF and pentane produces a film with 0.39–0.85 wt% W. The onset of polymerization, even at low temperatures, must limit defects (cross-linking and saturation) and permit the synthesis of temporarily soluble c-PA, which may be useful in device fabrication. Another unique feature of catalyst **1** is its exclusive reactivity with acetylene over ethylene. Exposing a benzene solution of catalyst **1** to a 4:1 mixture of acetylene/ethylene results in complete consumption of acetylene to produce c-PA. This result implies that ethylene streams used for the mass production of polyethylene and containing acetylene as a contaminant can be used to produce c-PA, thus effectively purifying the ethylene stream while at the same time producing high purity c-PA. The high-quality, low-defect films of c-PA produced with catalyst **1** reveal high electrical conductivity when doped with I_2. Since the c-PA forms in the >99% *trans* isomer, there is no need to subject the polymer to high temperatures, and the electrical conductivity observed (398 (±76) $\Omega^{-1}cm^{-1}$) is at the higher range of values reported for l-PA. The efficiency and selectivity of catalyst **1**, the pristine films produced, the temporarily soluble polymer afforded by the synthetic methodology, and the inherent differences of a cyclic topology should reinvigorate studies on PA in general, with perhaps a new focus on the physical properties implicated by a semiconducting cyclic polymer.

Online content

Any methods, additional references, Nature Research reporting summaries, source data, extended data, supplementary information, acknowledgements, peer review information; details of author contributions and competing interests; and statements of data and code availability are available at https://doi.org/10.1038/s41557-021-00713-2.

Received: 30 March 2020; Accepted: 26 April 2021;
Published online: 3 June 2021

References

1. Kekulé, A. Sur la constitution des substances aromatiques. *B. Mens. Soc. Chim. Paris* **3**, 98–110 (1865).
2. Kekulé, A. Ueber einige condensationsprodukte des aldehyds. *Ann. Chem. Pharm.* **162**, 77–124 (1872).
3. Lonsdale, K. The structure of the benzene ring in $C_6(CH_3)_6$. *Proc. R. Soc. Lond. A* **123**, 494–515 (1929).
4. Hückel, E. Quantentheoretische beiträge zum benzolproblem i. Die elektronenkonfiguration des benzols und verwandter verbindungen. *Z. Phys.* **70**, 204–286 (1931).
5. Rickhaus, M. et al. Global aromaticity at the nanoscale. *Nat. Chem.* **12**, 236–241 (2020).
6. Ni, Y. et al. 3D global aromaticity in a fully conjugated diradicaloid cage at different oxidation states. *Nat. Chem.* **12**, 242–248 (2020).
7. Sondheimer, F. & Wolovsky, R. The synthesis of cycloöctadecanonaene, a new aromatic system. *Tetrahedron Lett.* **1**, 3–6 (1959).
8. Sondheimer, F. & Gaoni, Y. Unsaturated macrocyclic compounds. XV. Ccyclotetradecaheptaene. *J. Am. Chem. Soc.* **82**, 5765–5766 (1960).
9. Kertesz, M., Choi, C. H. & Yang, S. Conjugated polymers and aromaticity. *Chem. Rev.* **105**, 3448–3481 (2005).
10. Yoshizawa, K., Kato, T. & Yamabe, T. Electron correlation effects and possible D_{6h} structures in large cyclic polyenes. *J. Phys. Chem.* **100**, 5697–5701 (1996).
11. Choi, C. H. & Kertesz, M. Bond length alternation and aromaticity in large annulenes. *J. Chem. Phys.* **108**, 6681–6688 (1998).
12. Natta, G., Mazzanti, G. & Corradini, P. *Atti Accad. Naz. Lincei Cl. Sci. Fis. Mat. Nat. Rend.* **25**, 3–12 (1958).
13. Chien, J. C. W. *Polyacetylene: Chemistry, Physics, and Material Science* (Academic, 1984).
14. Feast, W. J., Tsibouklis, J., Pouwer, K. L., Groenendaal, L. & Meijer, E. W. Synthesis, processing and material properties of conjugated polymers. *Polymer* **37**, 5017–5047 (1996).
15. Hudson, B. S. Polyacetylene: myth and reality. *Materials* **11**, 1–21 (2018).
16. Berets, D. J. & Smith, D. S. Electrical properties of linear polyacetylene. *Trans. Faraday Soc.* **64**, 823–828 (1968).
17. Shirakawa, H. & Ikeda, S. Infrared spectra of poly(acetylene). *Polym. J.* **2**, 231–244 (1971).
18. Chiang, C. K. et al. Synthesis of highly conducting films of derivatives of polyacetylene, $(CH)_x$. *J. Am. Chem. Soc.* **100**, 1013–1015 (1978).
19. Skotheim, T. A. & Reynolds, J. *Handbook of Conducting Polymers* (CRC, 2007).
20. Liu, J. Z., Lam, J. W. Y. & Tang, B. Z. Acetylenic polymers: syntheses, structures and functions. *Chem. Rev.* **109**, 5799–5867 (2009).
21. Nadif, S. S. et al. Introducing "ynene" metathesis: ring-expansion metathesis polymerization leads to highly *cis* and syndiotactic cyclic polymers of norbornene. *J. Am. Chem. Soc.* **138**, 6408–6411 (2016).
22. Gonsales, S. A. et al. Highly tactic cyclic polynorbornene: stereoselective ring expansion metathesis polymerization of norbornene catalyzed by a new tethered tungsten-alkylidene catalyst. *J. Am. Chem. Soc.* **138**, 4996–4999 (2016).
23. Xia, Y. et al. Ring-expansion metathesis polymerization: catalyst-dependent polymerization profiles. *J. Am. Chem. Soc.* **131**, 2670–2677 (2009).
24. Bielawski, C. W., Benitez, D. & Grubbs, R. H. An "endless" route to cyclic polymers. *Science* **297**, 2041–2044 (2002).
25. Chang, Y. A. & Waymouth, R. M. Recent progress on the synthesis of cyclic polymers via ring-expansion strategies. *J. Polym. Sci. Pol. Chem* **55**, 2892–2902 (2017).
26. Tezuka, Y. *Progress of Cyclic Polymers in Syntheses, Properties and Functions* (World Scientific, 2013).
27. McGowan, K. P., O'Reilly, M. E., Ghiviriga, I., Abboud, K. A. & Veige, A. S. Compelling mechanistic data and identification of the active species in tungsten-catalyzed alkyne polymerizations: conversion of a trianionic pincer into a new tetraanionic pincer-type ligand. *Chem. Sci.* **4**, 1145–1155 (2013).
28. Sarkar, S. et al. An OCO^{3-} trianionic pincer tungsten(VI) alkylidyne: rational design of a highly active alkyne polymerization catalyst. *J. Am. Chem. Soc.* **134**, 4509–4512 (2012).
29. Roland, C. D., Li, H., Abboud, K. A., Wagener, K. B. & Veige, A. S. Cyclic polymers from alkynes. *Nat. Chem.* **8**, 791–796 (2016).
30. Pal, D., Miao, Z. H., Garrison, J. B., Veige, A. S. & Sumerlin, B. S. Ultrahigh molecular weight macrocyclic bottlebrushes via post-polymerization modification of a cyclic polymer. *Macromolecules* **53**, 9717–9724 (2020).
31. Miao, Z. H., Kubo, T., Pal, D., Sumerlin, B. S. & Veige, A. S. pH-responsive water-soluble cyclic polymer. *Macromolecules* **52**, 6260–6265 (2019).
32. Niu, W. J. et al. Polypropylene: now available without chain ends. *Chem* **5**, 237–244 (2019).
33. Roland, C. D., Zhang, T., VenkatRamani, S., Ghiviriga, I. & Veige, A. S. A catalytically relevant intermediate in the synthesis of cyclic polymers from alkynes. *Chem. Commun.* **55**, 13697–13700 (2019).
34. Miao, Z. H. et al. Cyclic poly(4-methyl-1-pentene): efficient catalytic synthesis of a transparent cyclic polymer. *Macromolecules* **53**, 7774–7782 (2020).
35. Baker, G. L., Shelburne, J. A. & Bates, F. S. Preparation of low-spin *trans*-polyacetylene. *J. Am. Chem. Soc.* **108**, 7377–7380 (1986).
36. Ito, T., Shirakawa, H. & Ikeda, S. Simultaneous polymerization and formation of polyacetylene film on surface of concentrated soluble Ziegler-type catalyst solution. *J. Polym. Sci. Pol. Chem* **12**, 11–20 (1974).
37. Oth, J. F. M. Conformational mobility and fast bond shift in the annulenes. *Pure Appl. Chem.* **25**, 573–622 (1971).
38. Michel, C. S. et al. Tunneling by 16 carbons: planar bond shifting in [16] annulene. *J. Am. Chem. Soc.* **141**, 5286–5293 (2019).
39. Harada, I., Tasumi, M., Shirakawa, H. & Ikeda, S. Raman spectra of polyacetylene and highly conducting iodine-doped polyacetylene. *Chem. Lett.* **7**, 1411–1414 (1978).
40. Schugerl, F. B. & Kuzmany, H. Optical modes of *trans*-polyacetylene. *J. Chem. Phys.* **74**, 953–958 (1981).
41. Lichtmann, L. S., Fitchen, D. B. & Temkin, H. Resonant Raman spectroscopy of conducting organic polymers. $(CH)_x$ and an oriented analog. *Synth. Met.* **1**, 139–149 (1980).
42. Mulazzi, E., Brivio, G. P., Faulques, E. & Lefrant, S. Experimental and theoretical Raman results in *trans* polyacetylene. *Solid State Commun.* **46**, 851–855 (1983).
43. Ehrenfreund, E., Vardeny, Z., Brafman, O. & Horovitz, B. Amplitude and phase modes in *trans*-polyacetylene: resonant Raman scattering and induced infrared activity. *Phys. Rev. B* **36**, 1535–1553 (1987).
44. Kuzmany, H., Imhoff, E. A., Fitchen, D. B. & Sarhangi, A. Frank–Condon approach for optical-absorption and resonance Raman scattering in *trans*-polyacetylene. *Phys. Rev. B* **26**, 7109–7112 (1982).
45. Heller, E. J., Yang, Y. & Kocia, L. Raman scattering in carbon nanosystems: solving polyacetylene. *ACS Cent. Sci.* **1**, 40–49 (2015).
46. Chance, R. R., Schaffer, H., Knoll, K., Schrock, R. & Silbey, R. Linear optical-properties of a series of linear polyenes—implications for polyacetylene. *Synth. Met.* **49**, 271–280 (1992).
47. Schaffer, H. E., Chance, R. R., Silbey, R. J., Knoll, K. & Schrock, R. R. Conjugation length dependence of Raman scattering in a series of linear polyenes—implications for polyacetylene. *J. Chem. Phys.* **94**, 4161–4170 (1991).
48. Schaffer, H., Chance, R., Knoll, K., Schrock, R. & Silbey, R. Linear optical properties of a series of polyacetylene oligomers. In *Conjugated Polymeric Materials: Opportunities in Electronics, Optoelectronics, and Molecular Electronics* (eds Brédas, J. & Chance, R.) 365–376 (Springer, 1990).
49. Brivio, G. P. & Mulazzi, E. Theoretical analysis of absorption and resonant Raman scattering spectra of *trans*-$(CH)_x$. *Phys. Rev. B* **30**, 876–882 (1984).
50. Chen, Z. X. et al. Mechanochemical unzipping of insulating polyladderene to semiconducting polyacetylene. *Science* **357**, 475–478 (2017).
51. Kang, C., Jung, K., Ahn, S. & Choi, T. L. Controlled cyclopolymerization of 1,5-hexadiynes to give narrow band gap conjugated polyacetylenes containing highly strained cyclobutenes. *J. Am. Chem. Soc.* **142**, 17140–17146 (2020).
52. Gorman, C. B., Ginsburg, E. J. & Grubbs, R. H. Soluble, highly conjugated derivatives of polyacetylene from the ring-opening metathesis polymerization of monosubstituted cyclooctatetraenes—synthesis and the relationship between polymer structure and physical properties. *J. Am. Chem. Soc.* **115**, 1397–1409 (1993).
53. Scherman, O. A., Rutenberg, I. M. & Grubbs, R. H. Direct synthesis of soluble, end-functionalized polyenes and polyacetylene block copolymers. *J. Am. Chem. Soc.* **125**, 8515–8522 (2003).
54. Knoll, K. & Schrock, R. R. Preparation of *tert*-butyl-capped polyenes containing up to 15 double bonds. *J. Am. Chem. Soc.* **111**, 7989–8004 (1989).
55. Eckhardt, H. On the optical-properties of *trans*-polyacetylene. *J. Chem. Phys.* **79**, 2085–2086 (1983).
56. Sebelik, V. et al. Spectroscopy and excited state dynamics of nearly infinite polyenes. *Phys. Chem. Chem. Phys.* **22**, 17867–17879 (2020).
57. Fincher, C. R. et al. Electronic-structure of polyacetylene—optical and infrared studies of undoped semiconducting $(CH)_x$ and heavily doped metallic $(CH)_x$. *Phys. Rev. B* **20**, 1589–1602 (1979).
58. Leal, J. F. P. et al. Properties of charged defects on unidimensional polymers. *J. Comput. Theor. Nanosci.* **8**, 541–549 (2011).
59. Maricq, M. M., Waugh, J. S., Macdiarmid, A. G., Shirakawa, H. & Heeger, A. J. Carbon-13 nuclear magnetic resonance of *cis*- and *trans*-polyacetylenes. *J. Am. Chem. Soc.* **100**, 7729–7730 (1978).

60. Haberkorn, H., Naarmann, H., Penzien, K., Schlag, J. & Simak, P. Structure and conductivity of poly(acetylene). *Synth. Met.* **5**, 51–71 (1982).
61. Dubroca, T. et al. A quasi-optical and corrugated waveguide microwave transmission system for simultaneous dynamic nuclear polarization NMR on two separate 14.1 T spectrometers. *J. Magn. Reson.* **289**, 35–44 (2018).
62. Knoll, K., Krouse, S. A. & Schrock, R. R. Preparation and isolation of polyenes containing up to 15 double bonds. *J. Am. Chem. Soc.* **110**, 4424–4425 (1988).
63. Gibson, H. W., Kaplan, S., Mosher, R. A., Prest, W. M. & Weagley, R. J. Isomerization of polyacetylene films of the Shirakawa type—spectroscopy and kinetics. *J. Am. Chem. Soc.* **108**, 6843–6851 (1986).
64. Goldberg, I. B., Crowe, H. R., Newman, P. R., Heeger, A. J. & Macdiarmid, A. G. Electron-spin resonance of polyacetylene and AsF_5-doped polyacetylene. *J. Chem. Phys.* **70**, 1132–1136 (1979).
65. Weinberger, B. R., Kaufer, J., Heeger, A. J., Pron, A. & Macdiarmid, A. G. Magnetic susceptibility of doped polyacetylene. *Phys. Rev. B* **20**, 223–230 (1979).
66. Shirakawa, H., Ito, T. & Ikeda, S. Electrical properties of polyacetylene with various *cis–trans* compositions. *Makromol. Chem.* **179**, 1565–1573 (1978).
67. Bernier, P. et al. Magnetic properties of *cis*- and *trans*-polyacetylene as studied by electron spin resonance. *Polym. J.* **13**, 201–207 (1981).
68. Bernier, P. et al. Electronic properties of non-doped and doped polyacetylene films studied by ESR. *J. Phys. Lett.* **40**, L297–L301 (1979).
69. Heeger, A. J. Charge-transfer in conducting polymers. Striving toward intrinsic properties. *Faraday Discuss.* **88**, 203–211 (1989).
70. Pfeiffer, R. S., Yoder, G. & Chen, A. B. Ground state and excitations in polyacetylene chains. *Phys. Rev. B* **54**, 1735–1740 (1996).
71. Basescu, N. et al. High electrical conductivity in doped polyacetylene. *Nature* **327**, 403–405 (1987).
72. Tsukamoto, J. & Takahashi, A. Synthesis and electrical properties of polyacetylene yielding conductivity of 10^5 S/cm. *Synth. Met.* **41**, 7–12 (1991).
73. Doering, Wv. E. & Sarma, K. Stabilization energy of polyenyl radicals: all-*trans*-nonatetraenyl radical by thermal rearrangement of a semirigid {4-1-2} heptaene. Model for thermal lability of beta-carotene. *J. Am. Chem. Soc.* **114**, 6037–6043 (1992).
74. Bernardi, B. F., Garavelli, M. & Olucci, M. *Trans cis* isomerization in long linear polyenes as beta-carotene models: a comparative CAS-PT2 and DFT study. *Mol. Phys.* **92**, 359–364 (1997).

Data availability

All relevant data are provided in the figures, table and Supplementary Information.

Acknowledgements

A portion of this work was performed in the McKnight Brain Institute at the National High Magnetic Field Laboratory's Advanced Magnetic Resonance Imaging and Spectroscopy (AMRIS) Facility. The assistance from A. Mehta in the collection of the solid-state NMR data is gratefully acknowledged. D. Wei and J. Huang are acknowledged for assisting in the acquisition of diffuse-reflectance UV–vis spectra. This material is based on work supported by the National Science Foundation CHE-1808234. The solid-state NMR study was supported by National Science Foundation Cooperative Agreement DMR-1644779 and the State of Florida. The NMR spectrometer used to acquire the solid-state NMR spectra was funded, in part, by National Institutes of Health award S10RR031637. The MAS-DNP instrument at NHMFL is supported by the NIH P41 GM122698 and NIH S10 OD018519 grants.

Author contributions

Z.M. synthesized c-PA and l-PA in all forms, characterized c-PA and l-PA with IR, Raman, CP-MAS ^{13}C NMR and EPR, performed the cryogenic UV–vis monitoring the synthesis of temporarily soluble c-PA, synthesized and obtained the AFM images of cyclic bottlebrushes from temporarily soluble c-PA, and studied the conductivities of c-PA before and after doping with I_2. S.A.G. synthesized c-PA, characterized c-PA with IR and studied its conductivity. C.R.B. studied the CP-MAS ^{13}C NMR of c-PA and l-PA. C.E. provided data analysis and preliminary computational modelling of ^{13}C NMR data. F.M.-V. performed MAS-DNP ^{13}C NMR experiments. The manuscript was written with contributions from all authors. All authors have given approval to the final version of the manuscript. A.S.V. and B.S.S. directed the research.

Competing interests

The authors and UF Research Foundation Inc. have filed patents related to this subject matter. PCT Patent Application No. PCT/US21/17916.

Additional information

Supplementary information The online version contains supplementary material available at https://doi.org/10.1038/s41557-021-00713-2.

Correspondence and requests for materials should be addressed to B.S.S. or A.S.V.

Peer review information *Nature Chemistry* thanks the reviewers for their contribution to the peer review of this work.